Generating renewable power from water hammer pressure surges

A. Roberts[a,*], B. Thomas[a], P. Sewell[a], E. Hoare[a]

[a] *Department of Design and Engineering, Bournemouth University, Poole, Dorset, BH12 5BB*

Abstract

This article presents a system that makes use of the water hammer, which occurs when a fluid is subjected to a sudden change in momentum, to drive a piston-crank mechanism for power generation. Given that the magnitude of a water hammer is dependent upon the change in momentum experienced by the water, rather than the initial momentum itself, such a device may have applications operating as a pico scale hydropower device. The results of an experimental study are detailed, showing that a scale-model has a peak mechanical efficiency of 25.7 % and a mean efficiency of between 0.3 - 1.7 %. Potential applications for a refined version of the technology, namely pico-scale hydropower generation and energy recovery from surge tanks, are also discussed.

Keywords:

Pico hydropower, Water hammer, Hydraulic ram pump, Water hammer energy system, Hydraulic engine, Surge tank

*Corresponding author: robertsa@bournemouth.ac.uk

1. Introduction

1.1. Background and Motivation

In the context of climate change [1] and international targets on greenhouse gas emissions and global temperature increases [2], there is a pressing need to develop clean, renewable sources of energy. Unlike wind or solar, hydropower is one renewable energy source that is not as affected by issues such as producing variable and intermittent supplies. Even so, there are other drawbacks to hydropower, particularly at larger scales. These can include the amount of raw material required to construct large dams and the environmental and social damage that can be caused by flooding vast areas to create a reservoir [3, 4].

In many cases, the magnitude of these impacts is a function of the size of the system. In certain circumstances it is desirable to create smaller schemes that generate only a few kWs of power. Figure 1 summarises several different hydro technologies that can generate under 5 MW, along with with the input conditions they require. There is a gap towards the lower end of this scale, with few technologies that specifically target the low heads and flow rates that characterise pico (< 5 kW) generation.

Although pico generation is obviously very small scale, devices operating in this range can access a greater number of hydropower resources, and should be relatively cheap to install and maintain. They may therefore be of particular use in remote, developing, or rural areas where there is little capacity or need for larger, more complex infrastructure [6, 7]. Thanks to the relatively predictable and consistent nature of hydropower, these devices could also be of some use in micro-grids. These feature a variety of small

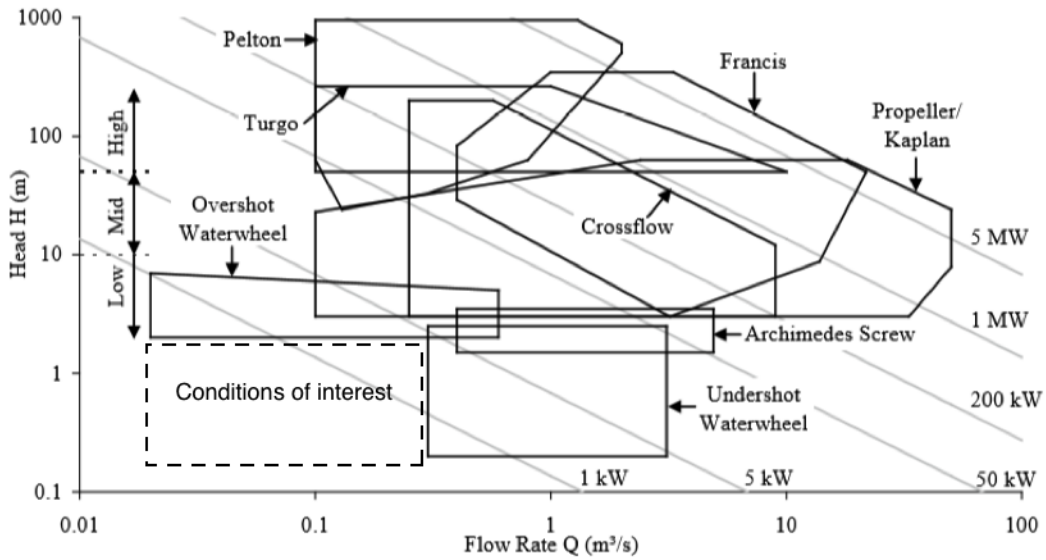

Figure 1: Application ranges of various hydropower devices. The highlighted area shows the conditions of interest that resulted in this work. Adapted from [5].

generation units instead of a large central plant, which provides some resilience against variable supplies. Since local resources can be accessed more readily, transmission losses can also be reduced, leading to improvements in efficiency and sustainability [8, 9].

The motivation underlying this research is to develop a cost-effective and reliable pico hydropower device, bearing in mind the potential uses and benefits it may bring in certain areas. The novel system presented here is an idea formulated during this work, and the concept may be of interest to those developing pico hydro schemes and technology, using hydraulic ram pumps, or designing piping systems.

1.2. *Power from the Water Hammer*

The water hammer occurs when a fluid is subjected to a sudden change in momentum, and is a form of unsteady flow characterised by sharp rises in pressure [10]. It commonly occurs in pipelines during valve operations, where it can cause problems such as noise, cavitation, and even total pipe failure in extreme cases [11]. The water hammer is therefore typically regarded as problematic, and most modern pipe systems employ surge tanks, slow closing valves, or other safety features to minimise its magnitude [12].

For an incompressible fluid where the valve closes slowly, rigid column theory provides a basic relation between the pressure surge Δp to the fluid density ρ, the pipe length l, and the rate of change of fluid speed $\frac{\mathrm{d}v}{\mathrm{d}t}$ [13]:

$$\Delta p = -\rho l \frac{\mathrm{d}v}{\mathrm{d}t} \tag{1}$$

If the valve closes rapidly, the compressibility of the fluid and pipe should be considered. In this case, the Joukowsky Equation [14] may be used to estimate Δp, which will be dependent upon the change in flow speed Δv, as well as the fluid density and sound speed c:

$$\Delta p = -\rho c \Delta v \tag{2}$$

In the UK, the terms water hammer and pressure surge are used interchangeably to describe both the compressible and incompressible phenomena. In North America the definitions are more strict: the term water hammer purely applies to flows that exhibit compressibility effects, while pressure surge does not, instead applying to unsteady flow caused by slower valve closures. The definition of slow or rapid valve closure is dependent upon the time t required by the pressure surge to propagate up the pipe, given by $t = l/c$.

1.2.1. Hydraulic Ram Pumps

Despite its potentially damaging effects, it is possible to harness the excess pressure of the water hammer for useful work. This is demonstrated by hydraulic ram pumps, which use the pressure generated by a periodically closing valve to pump water without an external fuel supply [15]. Hydraulic rams produce no greenhouse gas emissions during operation, are cheap to run, and are capable of operating passively for prolonged periods of time. This – combined with the reliability provided by possessing a limited number of moving parts (the valves themselves) – means that ram pumps are still employed in rural and developing regions, even though the principles of their operation have changed little since the 18th century [16].

An overview of the basic operation of a ram pump is provided in Figure 2. Water enters the drive pipe at the inlet (1) and flows through to the waste valve (4). The valve eventually slams shut due to the force of the water upon it (2), causing a rapid change in the momentum of the water within the drive pipe. The resulting excess pressure opens a delivery valve (5), where it is contained within a pressure chamber (6). This features a bleed valve to ensure there is a cushion of air within, which acts as a spring to force water up the delivery pipe to where it is required (3). Some of the pressure also propagates up the drive pipe to the inlet, causing the flow into the system to reverse due to the creation of a negative pressure gradient. This ultimately reduces the pressure within the system to such an extent that the delivery valve can close and the waste valve reopen, enabling the process to begin

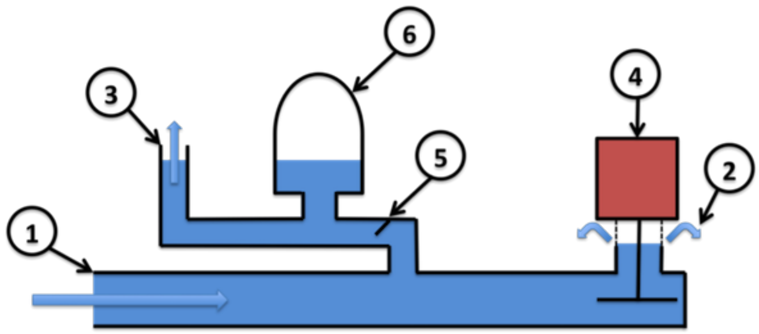

Figure 2: A basic overview of a hydraulic ram pump. (1) inlet, (2) valve outflow, (3) delivery pipe, (4) check valve, (5) delivery valve, (6) pressure chamber.

again.

1.2.2. The Water Hammer Energy System

Many water pumps are capable of operating as turbines for power generation [17]. With suitable modification, ram pumps are no exception. By replacing the delivery pipe and pressure vessel with an open standpipe – effectively creating a simple surge tank upstream of a periodically closing valve – it is possible to use the idea behind a ram to capture any excess pressure at the chamber [18]. The bulk of this pressure will be provided by the water hammer itself, however the level of the water in the chamber will also oscillate with the surge due to conservation of mass. This process is outlined in Figure 3. Several methods, as illustrated in Figure 4, could be used to extract energy from the chamber. These are a bi-directional Wells turbine (creating a system similar to an oscillating water column [19]), a linear alternator, or a mechanical linkage such as a piston-crank mechanism.

Given how similar this device is to a ram, it is reasonable to suppose that it may be capable of generating power in similar conditions. Whether

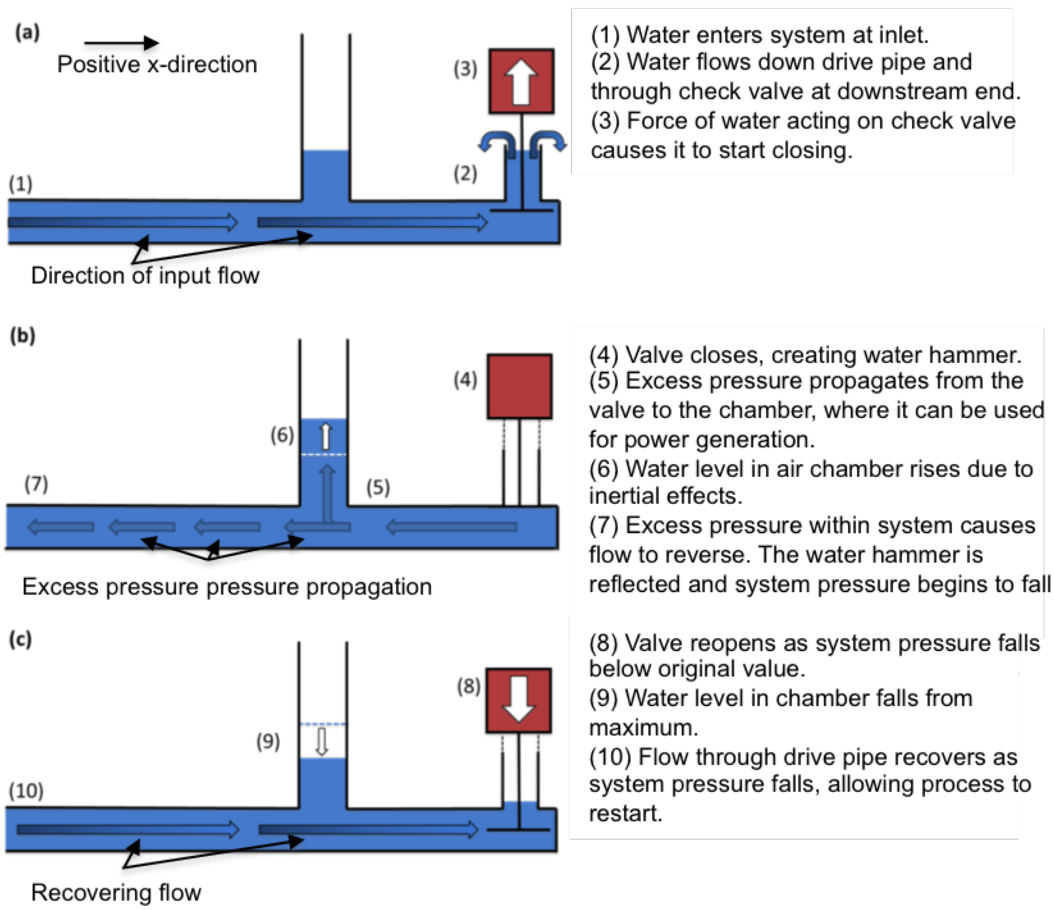

Figure 3: Overview of a water hammer energy system, neglecting the power take-off. The valve shown is for illustrative purposes only.

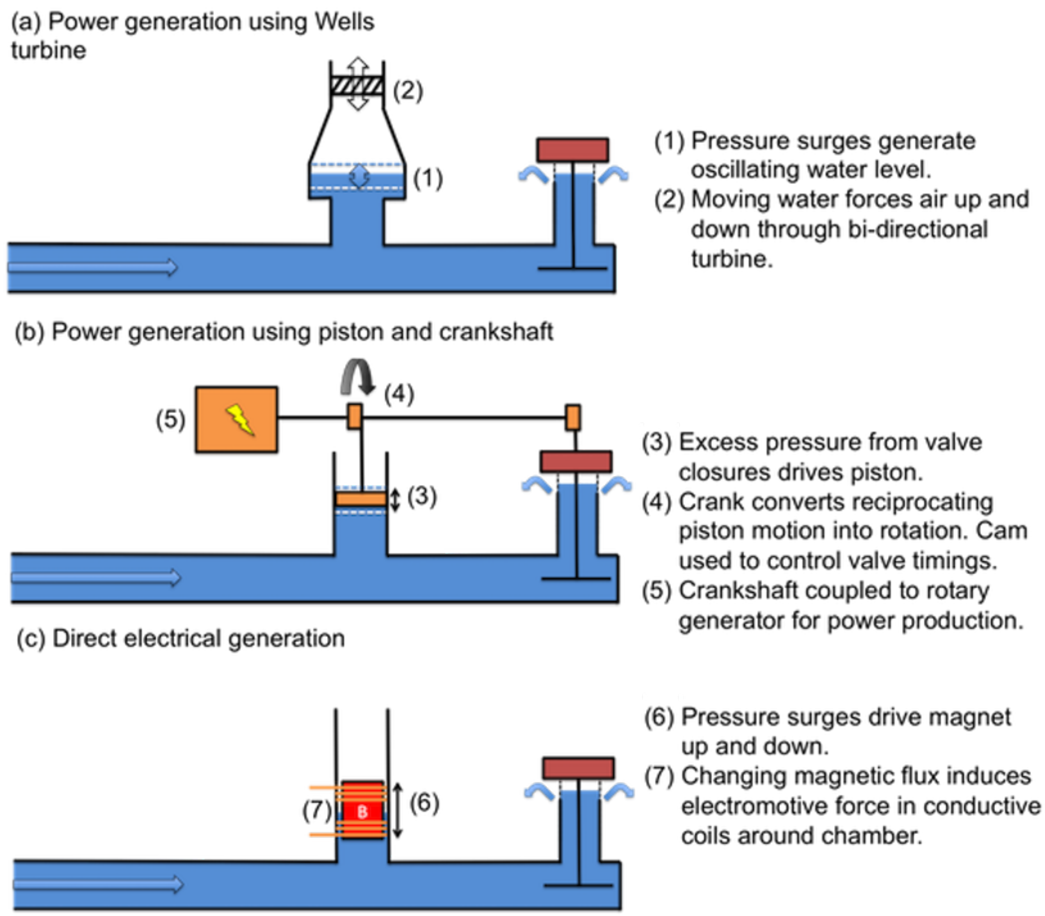

Figure 4: Suggested methods for generating power from a water hammer energy system: (a) Wells turbine, (b) piston-crank mechanism, (c) linear alternator.

or not doing this is worthwhile will depend upon the amount of energy it can provide, the reliability of the system as a whole, and how cost-effective it is (including how it fits in with any other utility systems) in comparison to other technologies. The first and third of these points will depend upon its efficiency, which will be governed by the magnitude of the pressure surges produced by each valve closure. Equations 1 and 2 show that this will be governed by the rate of change of momentum experienced by the fluid. This will depend not only on the available flow speed, but also upon the cross-sectional area and the length of the drive pipe. The length of the drive pipe is a crucial factor in the design of hydraulic ram pumps, with longer lengths providing greater pressure at the delivery outlet [20]. This suggests that a suitably designed water hammer energy system may be effective in relatively weak input conditions, as the flow rate will limit – but not directly govern – the amount of pressure the system can generate. An efficient water hammer system could therefore be an effective option for pico scale hydropower.

The remainder of this article presents the methods and results of an experimental study using a scale model water hammer energy system. The experiment consisted of measuring the performance of a piston-crank mechanism driven by a scale model test rig, with the aim of quantifying its efficiency to gain an initial indication of how effective such a system might be in a real world scenario. Some potential applications for the concept are then elaborated upon in the context of the experimental results.

2. Materials and Methods

2.1. Experimental test-rig

A rendered schematic of the experimental rig used in this study is provided in Figure 5.

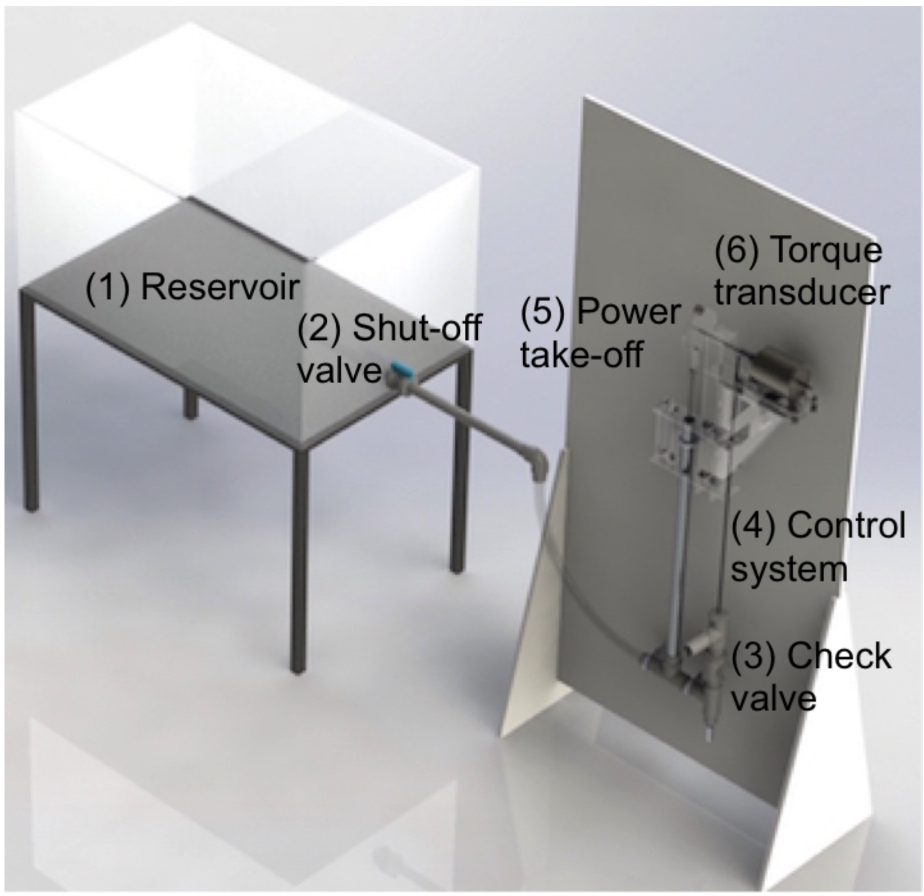

Figure 5: Render of the experimental test rig.

To facilitate easy modification, the test-rig was constructed from British Standard threaded sections of 20 mm diameter PVC pipe, which had a bore of 16 mm. The rig was driven by a reservoir of water with a maximum capacity of 0.084 m^3. This was located 0.35 m above the level of the 19 mm brass swing check valve that was used to generate the pressure surges, and was typically filled with around 0.20 m of water, providing a total input head of around 0.55 m, although this varied over the period of a test run for reasons described at the end of Section 2.2.

Given the flow rates that were measured during the experiment, this corresponds to an average input power of 0.75 - 1.60 W. The scale of the model and the input conditions were selected through a process of trial-and-error to reach a set-up that operated reliably. In comparison, the typical bore of commercial hydraulic ram pumps may vary from 50 to 150 mm with much larger designs also possible [21].

The check valve was actuated by a combination of the water flow and a push rod driven by a snail-drop cam connected to the crankshaft, which ensured that the valve closed at the correct crank angle. A schematic of this control system is shown in Figure 6, which highlights the return spring that was used to compensate for the weight of the push rod.

Unlike the rest of the rig, the vertical chamber was machined from an aluminium tube to ensure a tight fitting piston within. The piston itself was cut from acetyl to reduce any friction with the chamber walls. A superstructure made from laser-cut acrylic (for easy fabrication and consistent accuracy) was fitted onto the upper portion of the chamber, where it supported the crankshaft using Acetyl bushings. The crankshaft itself was made from 4 mm diameter stainless steel, while 4 mm diameter aluminium was used for the piston rod to reduce weight and minimise any issues with corrosion.

The crank, connecting rod, and cam were made from 3 mm thick laser-

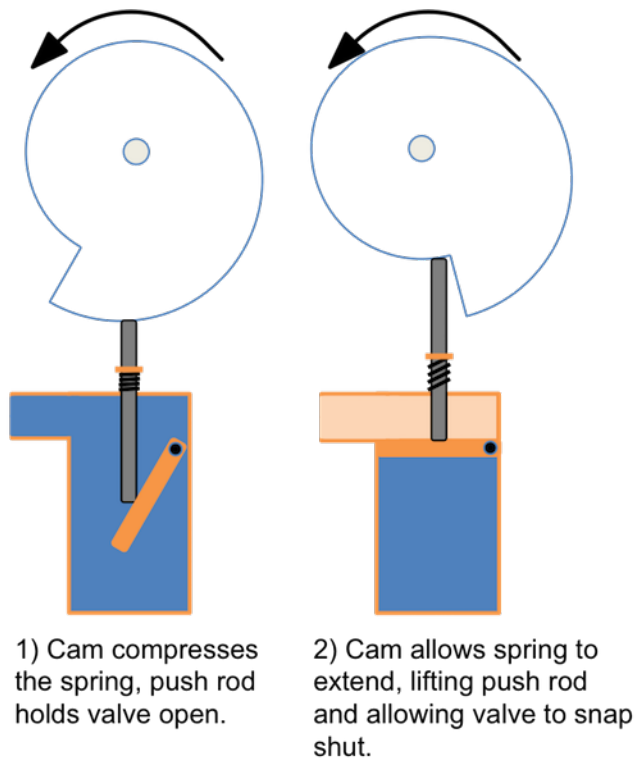

Figure 6: Schematic of the valve control system. The cam is located on the crankshaft. The size of the components is not to scale.

cut acrylic, again to enable rapid and accurate construction. The crank diameter of 75 mm was chosen according to the results of previous studies into the oscillatory amplitude of a piston within the chamber [22]. A 0.02 kg counterweight was attached to the crank opposite the piston rod fixing for balancing and additional inertia.

2.2. Instrumentation

A Sensor Technology ORT-241D Torque Transducer [23] was flexibly coupled to the crankshaft to measure the mechanical power generated by the crank. This sensor is capable of measuring up to 100 mNm of dynamic torque, and can handle a maximum shaft speed of 3×10^4 RPM. The sensor was connected via an RS232 cable to a laptop computer, which served as a data logger. A photograph of the test rig with the torque transducer attached is provided in Figure 7.

The transducer was activated several minutes before each set of experiments, so that the temperature of the instrumentation could stabilise. The transducer was coupled to a 3 V, 6:1 ratio gearbox motor, which was used to absorb the power generated by the crank. This was not used to control the shaft speed, since the noise of the power supplied by the motor masked that produced by the system. Instead, the system was allowed to behave according to the input conditions alone, with the unpowered motor acting as an additional load on the crankshaft.

To quantify the efficiency of the system, the power available from the reservoir was determined using four half-bridge load cells that were positioned underneath it. These were connected to a laptop computer via a 24-bit HX711 analogue to digital signal convertor and a 10-bit micro-controller. Following calibration, this enabled the mass of the reservoir to be measured as a function of time, enabling the variation in head and outflow rate – and by extension available power – to be determined. A drawback of this method was that the reservoir head diminished over the course of each test run.

2.3. Data analysis

The instantaneous power on the crank-shaft is computed as the product of the instantaneous torque τ and angular velocity ω measured by the transducer:

$$P(t) = \tau(t)\omega(t) \tag{3}$$

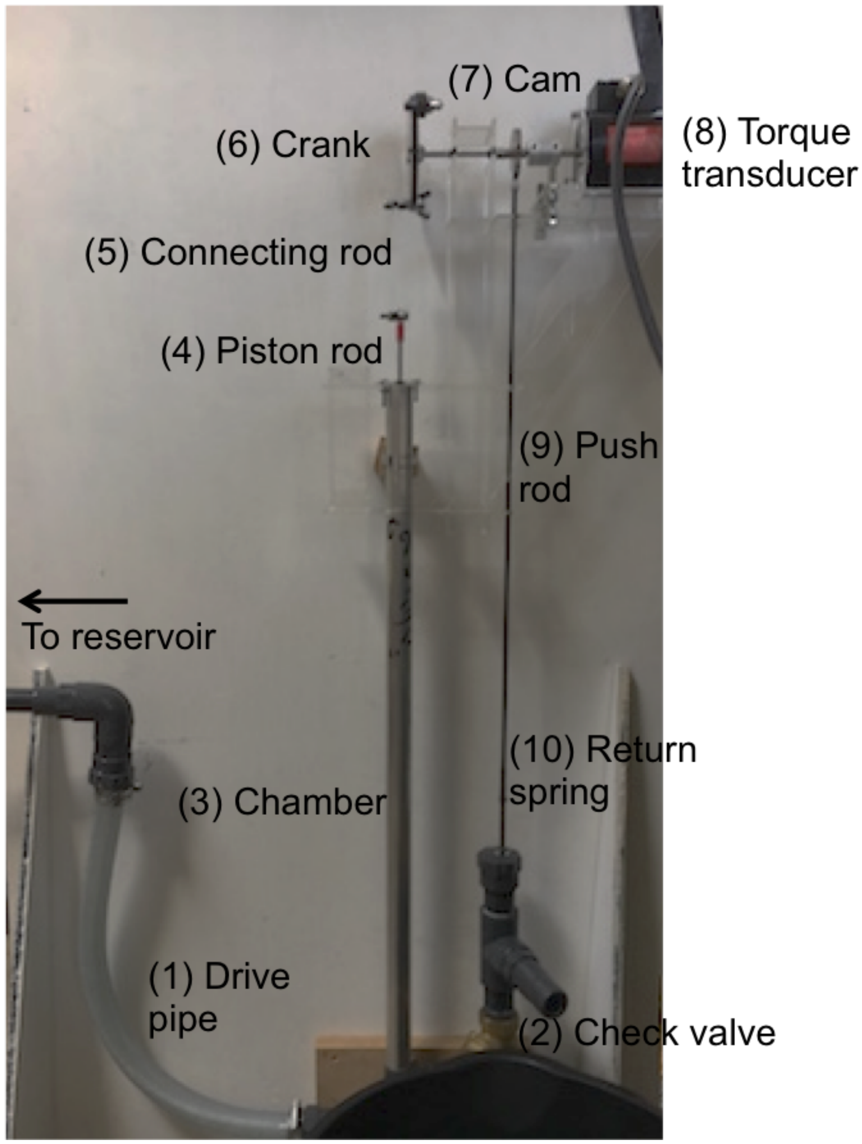

Figure 7: Photograph of the test-rig, including the chamber, valve control system, and torque sensor.

The average power available to the rig over a given period $\bar{P}_a$ is defined according to the mean reservoir head $\bar{h}$ and the mean mass flow rate $\bar{\dot{m}}$ over that period:

$$\bar{P}_a = \bar{\dot{m}} g \bar{h} \tag{4}$$

The mean efficiency of the system $\bar{\varepsilon}$ is defined as the percentage of the mean generated power $\bar{P}$ relative to the mean available power:

$$\bar{\varepsilon} = 100 \left(\frac{\bar{P}}{\bar{P}_a} \right) \tag{5}$$

In this study, $\bar{\varepsilon}$ provides an indication of how effective the system is at converting the power available in the flow into mechanical power on the crankshaft. If the system were being used to drive an electrical generator, further efficiency losses in the transmission and generator systems would need to be considered.

Due to the input head drop, each test was run for a period of 30 s, with the frequency of the valve closures varying according to the available input head and flow rate. To account for the diminishing reservoir head and subsequent variation in P_a, the data from each test run were subdivided into bins of approximately 4 s. The mean mass flow rate was computed for each of these periods by numerically differentiating the reservoir mass-time data and averaging the result, allowing time-averaged values of efficiency to be calculated.

Least squares fitting was used in attempt to quantify the correlation between certain variables. The curves that were fitted take the form of a power law, i.e. $y = ax^b$. For fitting this type of function to a series of n data points, the coefficients a and b can be calculated as follows:

$$a = \frac{\sum_{i=1}^{n} (\ln y_i) - b \sum_{i=1}^{n} (\ln x_i)}{n} \tag{6}$$

$$b = \frac{n\sum_{i=1}^{n}(\ln x_i \ln y_i) - \sum_{i=1}^{n}(\ln x_i)\sum_{i=1}^{n}(\ln y_i)}{n\sum_{i=1}^{n}(\ln x_i)^2 - (\sum_{i=1}^{n}(\ln x_i))^2} \tag{7}$$

The R^2 parameter, known as the coefficient of determination, is used to describe the validity of these curves:

$$R^2 = 1 - \frac{(\sum_{i=1}^{n} y_i - \hat{y}_i)^2}{(\sum_{i=1}^{n} y_i - \bar{y}_i)^2} \tag{8}$$

Here, $\hat{y}$ represents the value of y predicted by a model (i.e. the y value given by the curve) while $\bar{y}$ is the mean. An R^2 value of 1 indicates that the model perfectly predicts measured behaviour, while smaller values indicate that it is less accurate.

3. Experiment Results

3.1. Instantaneous data

Instantaneous values of torque and shaft RPM, as recorded by the torque transducer, are presented in Figure 8a and b, respectively. The data were recorded at a sample rate of 60 Hz, and were used to calculate the power curve that is shown in Figure 8c via Equation 3.

The measurement period shown includes three valve closure events. The water hammer generated by these closures is the cause of the abrupt spikes that are visible in all three curves; the excess pressure serving to kick the piston upwards and turn the crank over. This generates the bulk of the torque on the crank, however the water hammer are very short-lived, as they quickly dissipate through the system. As a result, although the mean peak torque on the shaft for the data shown in Figure 8a is 16.2 ± 2.11 mNm, the time-averaged torque over the period shown is much smaller at 0.45 ±

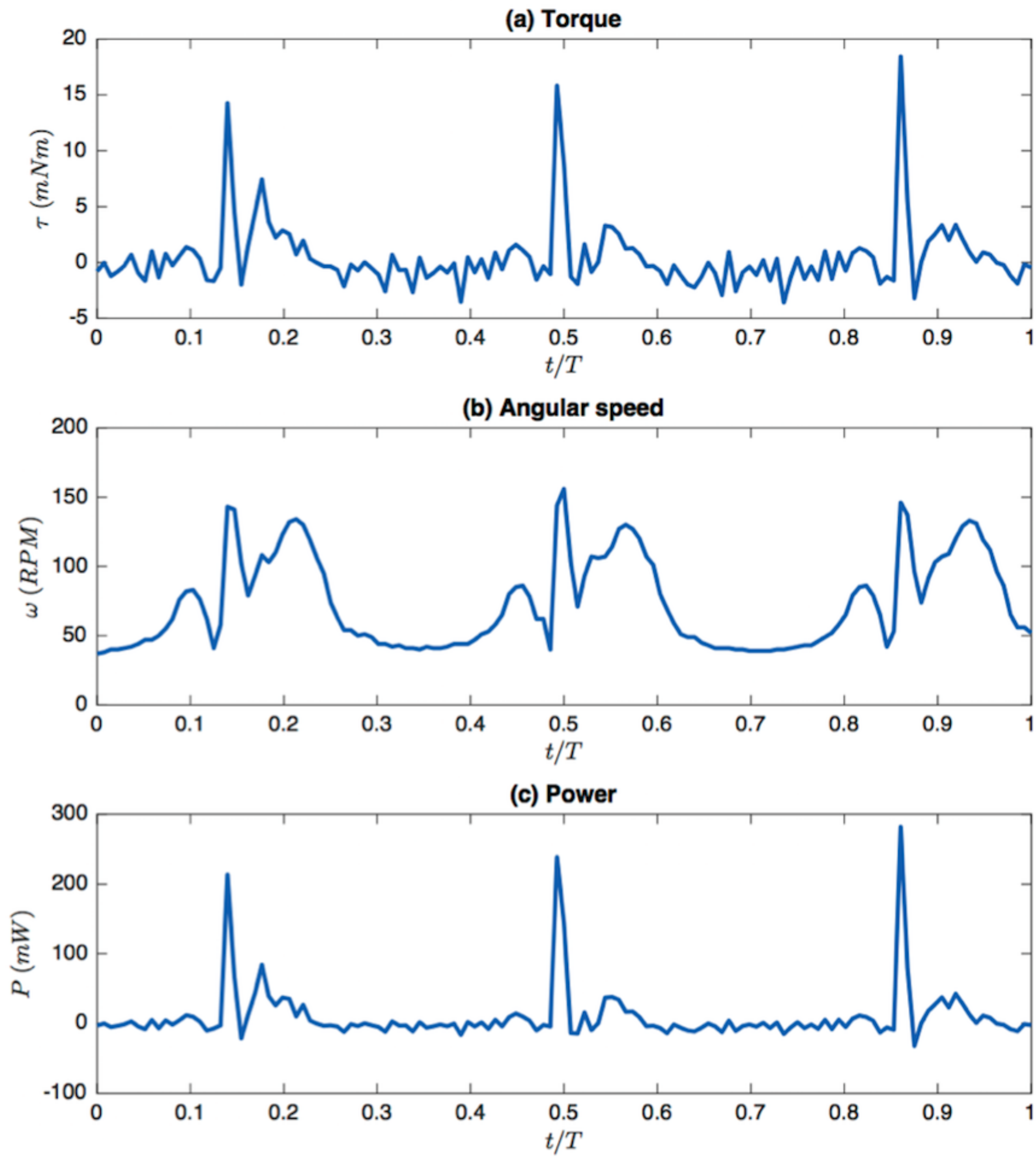

Figure 8: Example (a) torque (b) RPM and (c) power measurements across three valve closures.

3.04 mNm. The smaller, secondary peaks that occur after the main torque peaks in Figure 8a correspond to the remains of reflected pressure waves propagating through the system and acting on the piston, as well as the oscillating water level within the chamber due to the surges.

The torque pulses serve to accelerate the shaft to an angular speed that is significantly greater than the mean over a cycle. For Figure 8b, the mean peak shaft speed is 148 $\pm$ 6.81 RPM, compared to a time-averaged speed of 73.3 $\pm$ 33.0 RPM. Meanwhile, the lack of torque produced by the system on the downstroke, combined with the friction between the cam and the push rod actuating the valve, served to decelerate the shaft to a minimum speed of 38.6 $\pm$ 1.53 RPM.

The variable nature of the torque and shaft speed translates into large fluctuations into the power generated by the system. From Figure 8c, the peak power is generated when the water hammer is acting on the piston, which corresponds to when the torque and RPM are at their maximum. On average, the peak power is 244 $\pm$ 35.6 mW, a value that is 24 times greater than the mean value of 10.1 $\pm$ 41.3 mW. For this particular case, given the mean input head and mass flow rate of 0.57 m and 0.17 kg/s, the mean efficiency calculated via Equation 5 is 1.06 %. The mean peak efficiency, calculated by dividing the mean of the power peaks by the mean available power, was 25.7 %. This suggests that the system needs a more balanced power delivery, which could be achieved by adding additional cylinders or increasing the valve closure frequency.

3.2. Time-averaged data

Figure 9 shows the relationship between the mean power and the mean RPM of the shaft. The individual points represent time-averages of the instantaneous data taken over 4 s periods. This time span was chosen to balance the number of values used in the averages with the diminishing input head affecting device performance. The 27 data points consequently represent the number of complete, individual 4 s time periods available from the test runs conducted.

It can be seen that the time-averaged power increases with RPM. The fitted curve was computed using the least squares method described in Section 1.2. The trend shown in Figure 9 is ascribed to the more frequent valve closures that occur at higher RPMs, which increases the number of torque and power spikes in the instantaneous data over the period of the average. The valve closure frequency is dependent upon the balance of forces acting upon it – reducing the valve weight (or conversely increasing the force acting to close it) will enable it to close more frequently [18].

Figure 9 also shows that the average angular speed of the shaft ranged between 55 – 90 RPM over the course of the various test runs. Since the motor was not controlling the shaft speed, this variation is due to the changing speed and pressure of the water as it flowed through the check valve. This is highlighted more clearly in Figure 10, which shows the relationship between the RPM of the system and the input flow rate.

When the mean flow rate is slower, the amount of water within the chamber, as well as the forces acting on the check valve, will be lower [22]. This means the system has to do less work to hold the valve open and push the pis-

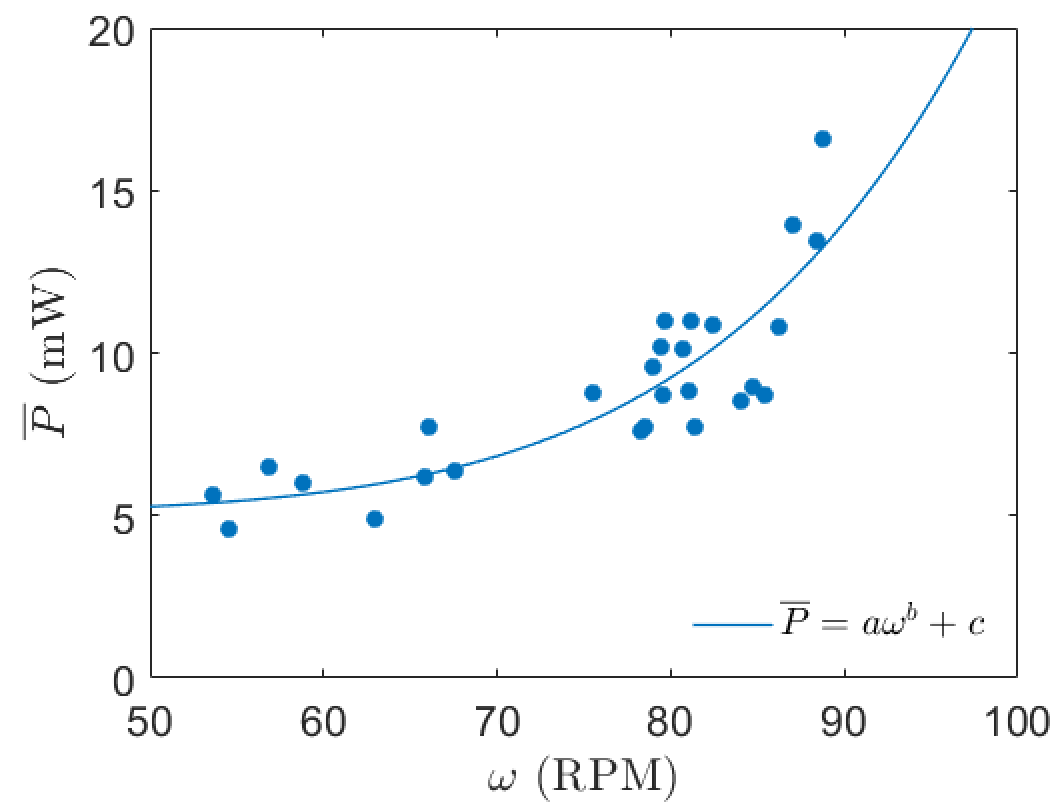

Figure 9: Relationship between mean cycle power and mean shaft RPM. The equation coefficients for the curve are $a = 1.88 \times 10^{-15}$, $b = 6.49$, and $c = 0.0051$. The R^2 value is 0.74.

ton down to bottom dead centre, allowing it to reach higher angular speeds. The fact that the valve is closing more frequently will also serve to choke the outflow rate [22], which will further reduce the resistance to the system completing a revolution.

The relationship between the mean efficiency of the system and the mean available power from the head and flow rate (calculated using Equation 4) is shown in Figure 11. Although the mean efficiency is low, it can be seen that

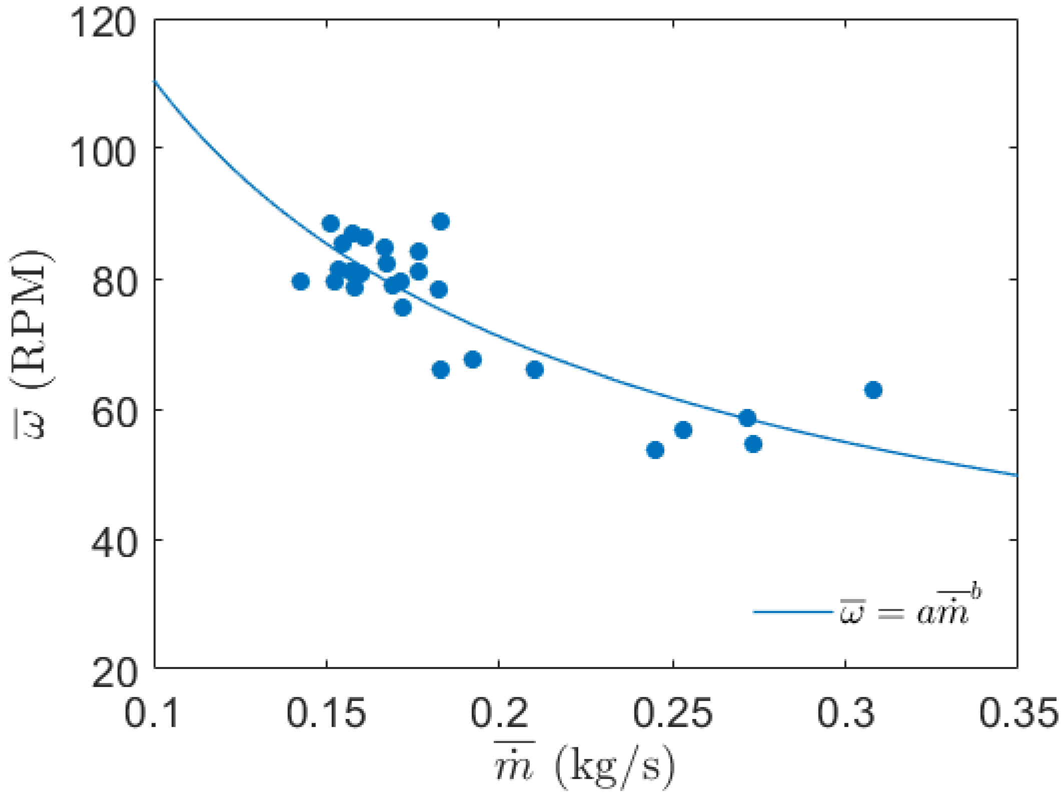

Figure 10: Relationship between input flow rate and system RPM. The equation coefficients for the curve are $a = 25.50$ and $b = -0.64$. The R^2 value is 0.74.

the system is at its most effective when less power is available.

The reason for this is again due to its mode of operation – in higher flow rates, when the valve is closing less frequently, more water is discharged through the valve between each closure, with the power available from this water being wasted. Conversely, when the valve is closing more frequently, less waste water is discharged between closures and more pressure and power spikes are generated over a given time. This again suggests that a higher frequency system may be optimal, although there will be a balance between

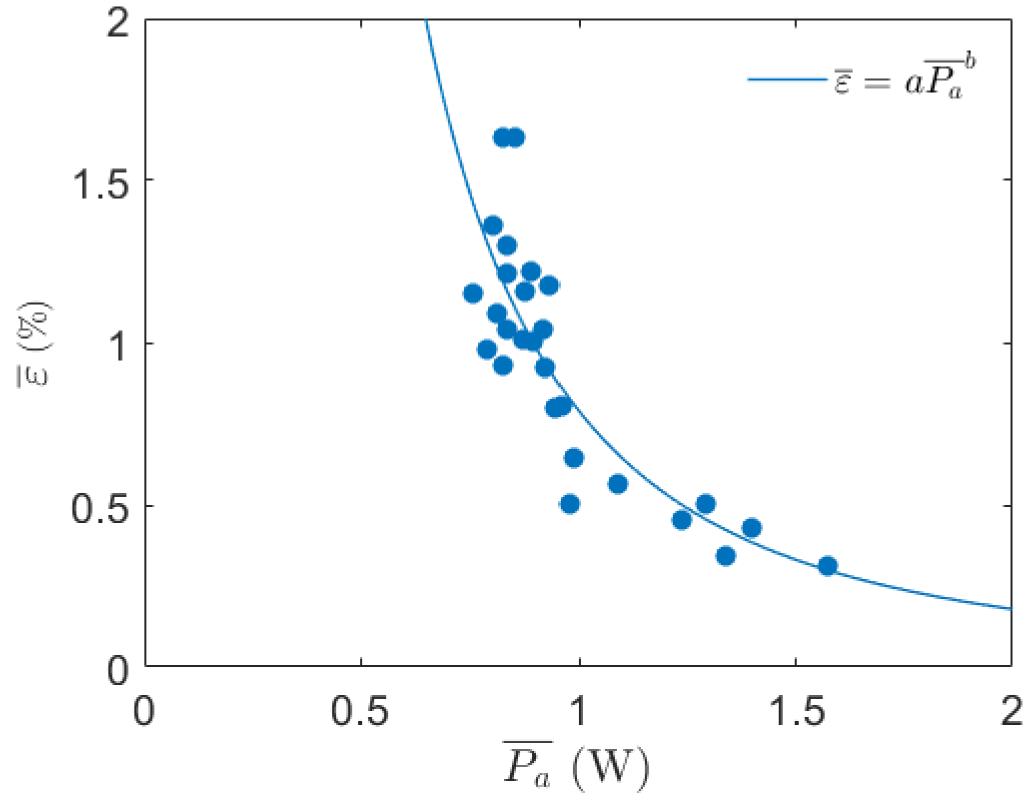

Figure 11: Relationship between mean system efficiency and available input power. The equation coefficients for the curve are $a = 0.79$ and $b = -2.15$. The R^2 value is 0.75.

the frequency of valve closures and the momentum change experienced by the water per closure event. Trade-offs such as this, as well as means to potentially improve the efficiency of the device, are discussed in the next section alongside potential applications.

4. Discussion of Potential Applications

4.1. Pico hydropower

Hydraulic ram pumps are chiefly employed in rural and remote areas. Given the similarities it has with these pumps, the water hammer energy system proposed in this article may be best employed in a similar manner – namely as a pico scale (i.e. < 5 kW) renewable generator for isolated or off-grid locations. Although the performance of the device could be improved in a number of ways (several of which are discussed below) the results presented in Section 3 indicate that this system is at best likely to operate at the low end of the pico-scale (i.e. < 1 kW). This is not only because of the relatively low power output of the scale model, but also because the results suggest that the most efficient system is likely to be operating at a high valve closure frequency in relatively weak input conditions.

Although the system as a whole is unproven, based on the performance of hydraulic rams, the underlying mechanism (i.e. the periodically closing valve) would at least be reliable. With this in mind, it could potentially be deployed in a wide variety of locations where low amounts of power are needed. In a similar vein to a conventional ram pump, the main requirement for its operation would be an available fall of water. Figure 12 provides an illustration of an envisaged set-up, with the water hammer energy system connected to a water source via a drive pipe. Such a system could be conceived for run-of-the-river generation or using water stored in a reservoir, using low input heads where other systems may be less suited.

The length of the drive pipe and the hydraulic head available to the system would be selected according to the requirements and specifics of an

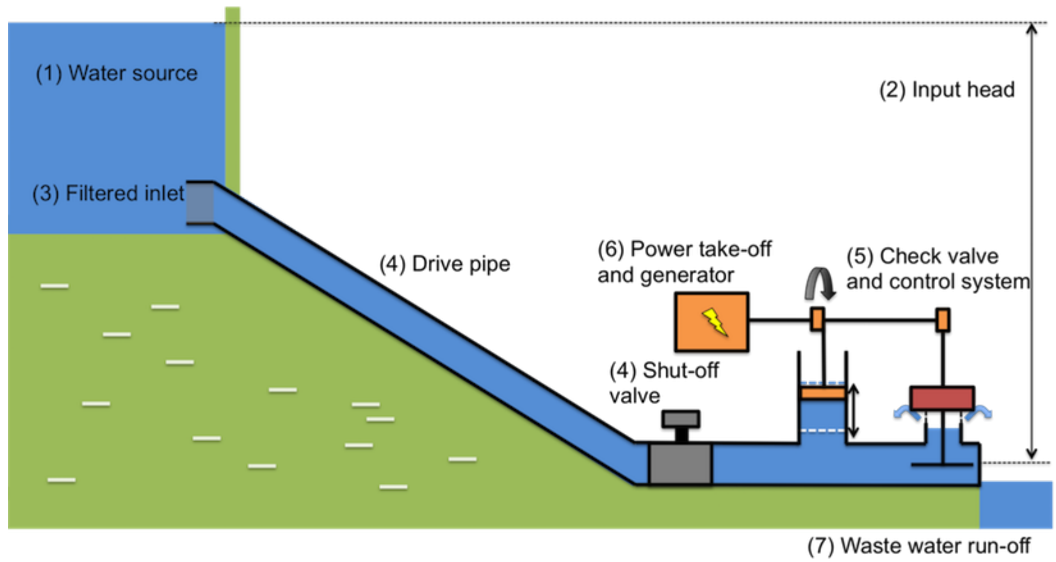

Figure 12: Envisaged set-up of water hammer energy system operating as a pico scale generator.

individual site. These would govern the power available from the device alongside the design (in terms of its size and valve behaviour). Provided there is enough water available, the energy system could operate alongside a conventional ram pump to provide both power and water storage. In this case, it may be desirable to use the generator to help purify the pumped water by powering an ultraviolet light in a purification system. A set-up along these lines could be highly beneficial in developing regions, and would help reduce the need for noisy, polluting, and expensive fossil fuel generators [24].

For this idea to be feasible however, higher values of efficiency and power output (compared to those of the scale model tested in this article) would need to be achieved. Depending on design and input conditions, hydraulic ram pumps can exhibit a wide range of efficiencies. For example, the designs described in [25] reached efficiencies of 13 - 15 % with a 1.8 m supply head, [26] reported an efficiency of 57 % with a 1.5 m supply head, [16] 44 % with a supply head of 9 m, and [20] 59.5 % in a 1.5 m supply head.

Whether these values are achievable for an energy system will be dependant upon input conditions, valve closure frequency, valve outflow rates, drive pipe length, and cross-sectional area. There will be trade-offs between maximising the valve closure frequency and the pressure available per surge. If the valve closes too frequently, then it may effectively start to choke the flow. This would reduce the momentum change that happens from one closure to the next, diminishing the pressure and power available. If it closes too infrequently however, then water will be wasted between each closure, and while the pressure from each surge may be maximised, the time-averaged power and efficiency will fall.

The control mechanism and the time required for the valve to shut will be a crucial factor in optimising this balance. The scale model tested here used a basic swing check valve, whereas commercial ram pumps use deformable rubber valves that are purposely designed to close as rapidly possible [27]. Altering this aspect of the design would likely enable more power to be generated per surge. Changing the material of the system, from the flexible PVC used in the scale-model shown here to something more rigid, would also allow more of the pressure generated by each valve closure to be captured, as less energy would be dissipated into the pipe walls.

Increasing the momentum of the water being stopped by the valve would also allow more power to be generated. This could be achieved by increasing the cross-section of the device and the length of the drive pipe. Doing this would also affect the balance of forces on the valve: a greater weight of water would help the valve close more quickly, however it would also increase the amount of work required for the timing system to ensure it reopened. All of these parameters should be assessed through numerical modelling involving the solution of the dynamic water hammer equations, which have not been presented here. There would certainly be trade-offs between the valve used and the momentum of the water flowing through the device.

A final option to increase the power output would be to improve the design of the power take-off itself. For the mechanical system demonstrated here, multiple pistons and a flywheel could be connected to a single crankshaft, much like an internal combustion engine. This would help smooth out power delivery by generating more torque pulses per crank revolution. In practice, other options may be more reliable, particularly the linear alternator. Direct electrical generation would reduce the number of moving parts and therefore the amount of maintenance required to keep a device operating effectively.

4.2. Energy capture in surge tanks

Another potential use for the idea behind this device may lie in conventional hydropower systems. As stated in Section 1.2, without its power take-off the water hammer energy system is effectively a simple surge tank, i.e. an open standpipe upstream of a valve. These are already used in a wide array of conventional piping systems to minimise and mitigate the effects of water hammer events. Figure 13 shows a schematic of a typical conventional hydropower set-up, based on that presented in [10], with the surge tank being used as an additional generator to capture some of the power in any pressure waves generated at the turbine.

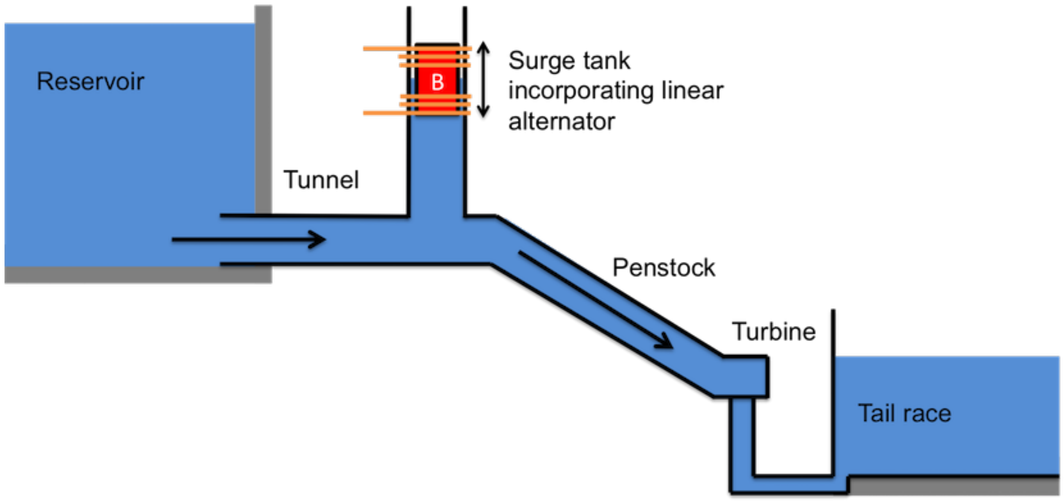

Figure 13: Schematic showing a surge tank combined with a linear alternator in a conventional hydro plant.

Given the potentially variable nature of the amplitude and frequency of water hammer events in this scenario, the mechanical power take-off that is the focus of this work may not be particularly appropriate. A linear alternator could be more suitable, since it would not require a consistent stroke length and may be more reliable. Proof that this concept is capable of generating electricity has previously been demonstrated in [22] for a system with a periodically closing valve. Numerical modelling work, via the solution of the momentum and mass equations that predict surge tank behaviour, should be conducted to assess the feasibility of this application.

5. Conclusions

This article has presented a method for generating mechanical power from the water hammer. By positioning a piston-crank mechanism upstream of a periodically closing valve, and using a cam to ensure the valve closes at the correct crank angle, it is possible to generate sufficient torque to turn over a crankshaft, providing a renewable source of mechanical power. Some potential applications for this system have been proposed, for example pico hydropower generation in remote or developing areas, however there would need to be considerable refinement of the current design to increase efficiency to a point where it could be viable.

The methods and results of a scale-model experiment into the effectiveness of a micro-hydropower system have also been discussed. Although the mean efficiency of the tested system was found to be low – ranging from between 0.3 to 1.7 % – the peak efficiency of the system was much larger at around 25 %. The peak efficiency value occurs immediately after a valve closure, when the water hammer kicks the piston upwards, providing a sharp burst of torque on the crank. Increasing the frequency of the valve closures – and hence the frequency of the water hammer – was found to increase the mean efficiency of the system. Since the closure frequency of the valve was governed by the input conditions, the available head and flow rate to the scale model also affected efficiency. Weaker input provided a greater mean efficiency, which suggests that such a system may be capable of operating in a wide range of conditions and locations if an efficient design can be developed.

6. Acknowledgements

The authors gratefully acknowledge Bournemouth University and the Balmain Environment Conservation Trust for funding this research project.

7. References

[1] IPCC, Climate Change 2013: The Physical Science Basis. Contribution of Working Group I to the Fifth Assessment Report of the Intergovernmental Panel on Climate Change, Cambridge University Press, Cambridge, United Kingdom and New York, NY, USA, 2013.

[2] UN, Adoption of the paris agreement, `https://unfccc.int/resource/docs/2015/cop21/eng/l09r01.pdf` (2015).

[3] F. Ligon, W. Dietrich, W. Trush, Downstream Ecological Effects of Dams, BioScience 45 (3) (1995) 183–192.

[4] L. Heming, P. Waley, P. Rees, Reservoir resettlement in china: past experience and the three gorges dam, The Geographical Journal 167 (3) (2001) 195–212.

[5] S. Williamson, B. Stark, J. Booker, Low Head Pico Hydro Turbine Selection using a Multi-Criteria Analysis, in: World Renewable Energy Congress 2011, Linköping, Sweden, 2011, pp. 1377–1385.

[6] A. Kadier, M. Kalil, M. Pudukudy, H. Abu Hasan, A. Mohamed, A. Hamid, Pico hydropower (PHP) development in Malaysia: Potential, present status, barriers and future perspectives 81 (2018) 2796–2805.

[7] S. Gladstone, V. Tersigni, K. Francfort, J. A. Haldeman, Implementing pico-hydropower sites in rural rwanda, Procedia Engineering 78 (2014) 279–286.

[8] M. Wolsink, The research agenda on social acceptance of distributed generation in smart grids: Renewable as common pool resources, Renewable and Sustainable Energy Reviews 16 (1) (2012) 822–835.

[9] J. Aghaei, M. Alizadeh, Demand response in smart electricity grids equipped with renewable energy sources: A review, Renewable and Sustainable Energy Reviews 18 (2013) 64–72.

[10] M. Chaudhry, Applied Hydraulic Transients, Springer, 2014.

[11] C. Bonin, Water-hammer damage to Oigawa power station, Journal of Engineering for Power 82 (2) (1960) 111–116.

[12] M. S. Ghidaoui, M. Zhao, D. A. McInnis, D. H. Axworthy, A review of water hammer theory and practice, Applied Mechanics Reviews 58 (1) (2005) 49–76.

[13] D. J. Stephenson, Pipeflow Analysis, Elsevier Science, 1984.

[14] N. Joukowsky, Uber den hydraulischen stoss in wasserleitungsro hren. (on the hydraulic hammer in water supply pipes), Memoires de l'Academie Imperiale des Sciences de St.-Petersbourg 8 (9).

[15] B. Young, Design of hydraulic ram pump systems, Proceedings of the Institution of Mechanical Engineers, Part A: Journal of Power and Energy 209 (4) (1995) 313–322.

[16] M. Inthachot, S. Saehaeng, J. F. Max, J. Müller, W. Spreer, Hydraulic ram pumps for irrigation in northern thailand, Agriculture and Agricultural Science Procedia 5 (2015) 107–114.

[17] M. Kramer, K. Terheiden, S. Wieprecht, Pumps as turbines for efficient energy recovery in water supply networks, Renewable Energy 122 (2018) 17–25.

[18] A. Roberts, B. Thomas, P. Sewell, N. Aslani, S. Balmain, I. Balmain, J. Gillman, The potential of the water hammer in pico-scale tidal power systems: An experimental investigation, in: Environment Friendly Energies and Applications (EFEA), 2016 4th International Symposium on, IEEE, 2016, pp. 1–6.

[19] A. F. Falcão, J. C. Henriques, Oscillating-water-column wave energy converters and air turbines: A review, Renewable Energy 85 (2016) 1391–1424.

[20] S. Sampath, S. Shetty, A. Mathew, W. Javaid, C. Selvan, Estimation of power and efficiency of hydraulic ram pump with re-circulation system, International Journal of Computer-aided Mechanical Design and Implementation 1 (1) (2015) 7–18.

[21] Green, Carter, Green and Carter Products Overview, `http://www.greenandcarter.com/main/products.htm` (2018).

[22] A. Roberts, The hydrodynamics of the water hammer energy system, Ph.D. thesis, Bournemouth University (2017).

[23] Sensor Technology, Rotary Torque Transducers and Wireless Load Sensors, https://www.sensors.co.uk (2017).

[24] C. Luijten, E. Kerkhof, Jatropha oil and biogas in a dual fuel ci engine for rural electrification, Energy Conversion and Management 52 (2) (2011) 1426–1438.

[25] N. Hussin, S. Gamil, N. Amin, M. Safar, M. Majid, M. Kazim, N. Nasir, Design and analysis of hydraulic ram water pumping system, in: Journal of Physics: Conference Series, Vol. 908, IOP Publishing, 2017, p. 012052.

[26] N. Shuaibu, Design and construction of a hydraulic ram pump, Leonardo Electronic Journal of Practices and Technologies 1583 (2007) 59–70.

[27] Water Powered Technologies Ltd and Papa Ltd, How the Papa Pump operates, https://www.waterpoweredtechnologies.com/how_it_works/ (2018).